

Manuscript ID ZUMJ-2401-3089 (R2)

DOI 10.21608/ZUMJ.2024.259344.3089

**ORIGINAL ARTICLE****Complementary Effect of Diffusion MR Imaging and Single-Voxel 1H MR Spectroscopy Metabolites in Characterization of Sellar and Suprasellar Masses**Rania Mostafa Hassan<sup>1\*</sup>, Ahmed Sabry Ragheb<sup>1</sup>, Samia Ali Taher Elmajdub<sup>2</sup>, Rania M Almolla<sup>1</sup>

1- Radiodiagnosis Department, Faculty of Medicine, Zagazig University, Egypt

2- Radiodiagnosis Department, Tripoli Central Hospital, Tripoli, Libya

**\*Corresponding author:**

Rania Mostafa Hassan\*

Radiodiagnosis Department,  
Faculty of Medicine, Zagazig  
University, Egypt**Email:**[Raniahassan@medicine.zu.edu.eg](mailto:Raniahassan@medicine.zu.edu.eg)[Ronina7@hotmail.com](mailto:Ronina7@hotmail.com)

Submit Date 2024-01-06

Revise Date 2024-01-22

Accept Date 2024-01-24

**ABSTRACT**

**Background:** Sellar and suprasellar regions are complex areas of the brain, where different varieties of lesions can occur in this confined space. When evaluating sellar and suprasellar lesions prior to surgery, diffusion weighted MRI and MR spectroscopy are regarded as crucial diagnostic tools that supplement conventional MRI.

**Aim of the Study:** The aim of the recent study was to evaluate the role of the DWI and Single-Voxel 1H MRS Metabolites in characterization of Sellar and Suprasellar masses.

**Methods:** A prospective study has been conducted on 30 patients with various sellar and suprasellar masses consulted from Neurosurgery and Neurology Departments to the MRI unit over a period of 6 months between June 2023 and Nov 2023. They were examined with long-echo single voxel 1H -MRS and DWI by 1.5 Tesla clinical imaging machine. Examinations were guided by cMRI. We confirmed our diagnosis pathologically after surgical management.

**Results:** Sellar and suprasellar tumors exhibited variable values for diffusion and the mean ADC value was for macroadenoma is  $(0.72 \pm 0.25) \times 10^{-3}$  mm<sup>2</sup>/sec, craniopharyngeoma is  $(1.8 \pm 0.1) \times 10^{-3}$  mm<sup>2</sup>/sec, glioma is  $(1.38 \pm 0.5) \times 10^{-3}$  mm<sup>2</sup>/sec, germinoma  $(0.80 \pm 0.2) \times 10^{-3}$  mm<sup>2</sup>/sec and for meningioma is  $(0.94 \pm 0.16) \times 10^{-3}$  mm<sup>2</sup>/sec. Pituitary macroadenoma were typically characterized by Cr peak, moderate elevation of Cho peak and significant reduction of NAA. Craniopharyngiomas were classically distinguished by notable reduction of all metabolites. Rise of Cho peak and decrease of NAA and Cr peaks typically characterize Gliomas. The most distinguishing metabolite of meningioma is Alanine.

**Conclusions:** Diffusion-weighted MRI and MR Spectroscopy can contribute to presurgical assessment and discrimination between various sellar, suprasellar masses.

**Keywords:** Sellar; Suprasellar ; MR spectroscopy; ADC value.

**INTRODUCTION**

Despite decades of progress, the identification of diseases affecting the sellar and suprasellar regions is still the most challenging due to their intricate structure and varied disorders. When characterizing masses with MRI, signal intensity, contrast enhancement form and lesion morphology, are considered into account. However, even when the data are assessed collectively, diverse sellar and

suprasellar diseases may still be difficult to distinguish from one another [1].

When evaluating sellar and suprasellar lesions prior to surgery, magnetic resonance spectroscopy (MRS) and diffusion weighted MRI (DWI) are thought to be crucial diagnostic tools that supplement conventional MRI [2,3,4].

DWI is a widely available non-invasive functional MR imaging technique. It aids in the

assessment of tissue features depending on the movement of water protons within the tissue. A mass can be quantitatively evaluated by computing its apparent diffusion coefficient (ADC) value, which has an inverse relationship with tissue cellularity. [5, 6, 7].

In many common neurological illnesses, 1H-MRS is becoming more and more significant when used in conjunction with structural imaging modalities. Only a small number of published 1H-MRS research addressed sellar and suprasellar neoplasms, while the majority of investigations examined parenchymal brain lesions [2].

The current study was aiming to appraise the role of the DWI and Single-Voxel 1H MRS Metabolites in characterization of Sellar and Suprasellar masses.

### METHODS

The current prospective study has been performed on 30 patients; they were conveyed from Neurosurgery and Neurology Departments to the MRI unit in the Radiodiagnosis Department, over a period of 6 months in the time setting between June 2023 and Nov 2023.

#### *Ethical consent:*

Academic and Ethical Committee of Zagazig University approved the study (IRB #10738). Every patient consented to participate in the recent study by a written informed consent. The Declaration of Helsinki, the World Medical Association's code of ethics for research involving human subjects, guided the conduct of this study.

*We included* any patient with sellar and suprasellar lesions detected by cMRI. Also any age group and both sexes are included.

*Patient exclusion criteria includes* patients who have contraindication for MRI (implanted electronic and electric devices, heart pacemakers, implanted hearing aids, insulin pumps and intracranial metal clips), patients previously operated with both sellar and /or suprasellar residual lesions, patients having pituitary microadenomas, patients who did not have histopathological result and patients who refused to complete the study.

#### *Patient preparation:*

Every patient was requested to remove any metallic objects from their bodies and was questioned about any conditions that might preclude an MRI (such as an artificial heart valve, metallic stent, joint prosthesis other than titanium, or cardiac pacemaker). The length of the examination, the patient's position, and the significance of remaining still were all explained to the patients.

#### *Sequences:*

All investigations were held using 1.5 Tesla clinical machine (General electronics Signa Excite and Philips Medical System -Achiva-class II, USA) with a standard head coil. The following protocol was used:

(1) Non contrast axial, sagittal and coronal T1WIs (TE 15 m/s, TR 400–550 m/s, matrix 256 \*256, FOV 250, section thickness 3 mm, interslice gap 1 mm).

Axial T2WI (TE 110 m/s, TR 3500–4800 m/s, FOV250, slice thickness 3 mm, matrix 256\*256, interslice gap 1 mm).

(2) Post contrast sagittal and coronal T1WI after administration of gadolinium 0.1 mm/kg body weight.

(3) Breath hold DWI was done before contrast agent administration, with a single-shot spin-echo echo-planner sequence (FOV 38 cm, TR/TE: 2000/33–55, section thickness 6 mm, matrix size 128 \*128, interslice gap 1 mm, b values 0 and 1000 s/mm<sup>2</sup>).

(4) ADC values were measured by using circumferential ROI (8–50 mm<sup>2</sup>) in the central and solid appearing portions of lesions and ADC maps were calculated automatically.

(5) Single-voxel spectroscopic examinations were guided by cMRI. The rectangular 1H-MRS voxel was put on the solid part of the tumor with averting of contamination with skull and cerebral ventricles, also avoiding its necrotic / cystic areas. Acquisition of the spectrum was by Stimulated Echo Acquisition Mode (STEAM). The size of the voxel utilized was either 20 x 20 x 20 mm (volume: 8 cc) or 15 x 15 x 15 mm (volume: 3.4 cc).

We obtained metabolite signals from choline-containing compounds (Cho), N-acetylaspartate (NAA), creatine (Cr), lactate (Lac), and mobile lipids (Lip), centered, at 3.2, 3.0, 2.0, 1.3, and 0.9 ppm respectively. We evaluated qualitatively the presence of each metabolite peak by visual inspection and type of the pathological 1H-MR spectra was determined according to the classification as shown in (Table 1) Chernov et al [8].

#### *Reference standard:*

We confirmed our diagnosis pathologically after surgical management.

#### *Statistical analysis:*

The collected data were computerized and statistically investigated using IBM SPSS 23.0 for windows (SPSS Inc., Chicago, IL, USA).

**RESULT**

Our study enrolled 30 patients. They were 14 females and 16 males; their ages were ranged from 4 to 55 years with mean age (mean= 32.1±16.1) (Table 2). Pituitary macroadenomas, craniopharyngioma, and chiasmatic-hypothalamic glioma were the major constituents for the study consisting of 50%, 16.7%, and 13.3% of the cases, respectively, followed by germinoma 10% and meningioma 10% (Table 3).

According to the clinical history, the main symptomatology was headache in (76.7%) of cases followed by visual disturbance in (53.3%) of cases (Table 2).

By c MRI most of macroadenoma lesions had well defined morphology and hyper-intense signal in T2W1 (66.7% and 73.3%) respectively. On diffusion imaging, the signal intensity was hypointense and hyperintense on ADC map and DWI respectively in (46.7%) cases. The ADC values measured on ADC map, ranging from (0.4-1.1) x 10<sup>-3</sup> mm<sup>2</sup>/s with mean ADC (0.72±0.25) x 10<sup>-3</sup> mm<sup>2</sup>/s. In our study 6 patients of macroadenoma (40%) had type IIC with moderate elevation of lip, 3 patients (20%) had type IA and IIC with mild lip elevation each, and only one patient (6.7%) had type IIIB (table 4).

Among 5 patients diagnosed with craniopharyngioma, (80%) had hyperintense signal in T1W1, all them (100%) had hyper-intense signal in T2W1. The DWI of craniopharyngiomas appeared hypointense with high ADC values in (80%) of cases, where the mean ADC values of craniopharyngiomas was (1.8 ± 0.1) 10—3 mm<sup>2</sup>/s. In our craniopharyngiomas cases we attained MR

spectra type IIIC in 3 cases (60%) and 2 patients (40%) had type IIC with moderate lip elevation (table 4).

Four patients with gliomas, (75%) of them had hypointense signal in T1W1 and all of them (100%) had hyperintense signal in T2W1. (50%) of gliomas were hypointense on DWI and hyperintense on ADC map with mean ADC (1.38±0.5) x10<sup>-3</sup> mm<sup>2</sup>/sec (table 4).

MR pathological spectra for our glioma cases were distinguished by increase of Cho peak ,decreased NAA, and Cr peaks. Three tumors had pathological 1H-MR spectra type II: (2 IIC with mild lip rise, one patient had type IIC with moderate lip elevation) and one patient had type IIIC (table 4).

All the 3 patients diagnosed with meningioma were well-defined homogenous enhancement and had isointense in both T1W1 and T2W. The mean ADC value in meningiomas was (0.94±0.16) x 10—3 mm<sup>2</sup>/s. with no diffusion restriction on DWI. Regarding MRS of meningioma 2 cases out of 3 as they showed type IIC spectrum with a rise in Alanine peak (at 1.49 ppm) while the third case revealed characteristic type IIC with no alanine peak(table 4).

Also, all the 3 patients diagnosed with germinoma had isointense signal in T1W1 and (66.7%) in T2W1, majority of them (66.7%) were hyperintense on DWI with average ADC values (0.80±0.2) 10—3 mm<sup>2</sup>/s. Among the three patients diagnosed with germinoma, 2 patients had type IIC with moderate lip elevation and one patient had type IIIA (predominant peak was Lip then Cho) (table 4).

**Table 1:** Determination of the type of pathological 1H-MRS: *Chernov et al., [8]*.

Type of the pathological 1H-MR spectra	Predominant metabolite Peak	Presence of Lac Peak	Presence of Lip peaks
Type I A	NAA (NAA content < 0.75 and/or Cho content > 1.25)	No	No
Type I B	NAA	Yes	No
Type I C with mild elevation of Lip	NAA	Not relevant	Yes (Lip/Cho < 1)
Type I C with moderate elevation of Lip	NAA	Not relevant	Yes (Lip/Cho > 1)
Type II A	Cho	No	No
Type II B	Cho	Yes	No

Type II C with mild elevation of Lip	Cho	Not relevant	Yes (Lip/NAA < 1)
Type II C with moderate elevation of Lip	Cho	Not relevant	Yes (Lip/NAA > 1)
Type III A	Lip (Cho peak preserved)	Not relevant	Yes
Type III B	Lip (significant reduction or disappearance of Cho peak)	Not relevant	Yes
Type III C	Absence of any detectable metabolite peak		

NAA, N-acetylaspartate; Cho, choline-containing compounds; Lac, lactate; Lip, mobile Lipids.

**Table 2:** Demographic and clinical data among studied patients

Variable	All patients (n=30)
<b>Age</b> mean±SD (range)	32.1±16.1 (4 – 55)
	<b>N. %</b>
< 10 years	5 (16.7%)
20 – 30 years	4 (13.3%)
30 – 40 years	2 (6.7%)
40 – 50 years	7 (23.3%)
50 – 60 years	6 (20%)
>60 years	6 (20%)
<b>Sex</b>	<b>N. %</b>
Male	16 (53.3%)
Female	14 (46.7%)
<b>Clinical data</b>	<b>All patients (n=30)</b> <b>(N. %)</b>
Headache	23 (76.7%)
Visual disturbance	16 (53.3%)
Recurrent vomiting	5 (16.7%)
Acromegaly	1 (3.3%)
Galactorrhea	1 (3.3%)
Diabetes insipidus	3 (10%)
Short stature	1 (3.3%)
Amenorrhea	3 (10%)

**Table 3:** Histopathology finding among studied patients

Histopathology findings	All patients (n=30) (N. %)
Macro adenoma	15 (50%)
Craniopharyngeoma	5 (16.7%)
Gliomas	4 (13.3%)
Germinoma	3 (10%)
Meningioma	3 (10%)

**Table 4:** cMRI , DWI , ADC and MRS findings in relation to different lesions

	<b>MA (n=15)</b>	<b>CP (n=5)</b>	<b>GL (n=4)</b>	<b>GM (n=3)</b>	<b>MG (n=3)</b>	<b>P-value</b>
<b>Morphology:</b>						
Well-defined	10(66.7%)	5(100%)	1 (25%)	3 (100%)	3 (100%)	0.07
Ill-defined	5 (33.3%)	0 (0%)	3 (75%)	0 (0%)	0 (0%)	
<b>T1W1:</b>						<b>0.01</b>
Iso-intense	6 (40%)	0 (0%)	1 (25%)	3 (100%)	3 (100%)	
Hypo-intense	6 (40%)	1 (20%)	3 (75%)	0 (0%)	0 (0%)	
Hyper-intense	3 (20%)	4 (80%)	0 (0%)	0 (0%)	0 (0%)	
<b>T2W1:</b>						<b>0.001</b>
Iso-intense	0 (0%)	0 (0%)	0 (0%)	2 (66.7%)	3 (100%)	
Hypo-intense	4 (28.6%)	0 (0%)	0 (0%)	0 (0%)	0 (0%)	
Hyper-intense	11(73.3%)	5 (100%)	4(100%)	1 (33.3%)	0 (0%)	
<b>DWI (b 100):</b>						0.2
Iso-intense	3 (20%)	0 (0%)	1 (25%)	1 (33.3%)	2 (66.7%)	
Hypo-intense	5 (33.3%)	4 (80%)	2 (50%)	0 (0%)	0 (0%)	
Hyper-intense	7 (46.7%)	1 (20%)	1 (25%)	2 (66.7%)	1 (33.3%)	
<b>ADC map:</b>						<b>0.03</b>
Iso-intense	3 (20%)	0 (0%)	2 (50%)	1 (33%)	3 (100%)	
Hypo-intense	7 (46.7%)	1 (20%)	0 (0%)	2 (66.7%)	0 (0%)	
Hyper-intense	5 (33.3%)	4 (80%)	2 (50%)	0 (0%)	0 (0%)	
<b>ADC value</b>						<b>0.04</b>
Mean±SD (range)	0.72±0.25 (0.4–1.1)	1.8±0.1 (1.7- 1.9)	1.38±0.5 (0.7-1.9)	0.80±0.2 (0.6-1)	0.94±0.16 (0.8-1.1)	
<b>MRS curve</b>						
<b>IA</b>	3 (20%)	0 (0%)	0 (0%)	0 (0%)	0 (0%)	<b>0.6</b>
<b>IIC (mild)</b>	3 (20%)	0 (0%)	2 (50%)	0 (0%)	1 (33.3%)	
<b>IIC (moderate)</b>	6 (40%)	2 (40%)	1 (25%)	2(66.7%)	2 (66.7%)	
<b>IIIA</b>	0 (0%)	0 (0%)	0 (0%)	1(33.3%)	0 (0%)	
<b>IIIB</b>	1(6.7%)	0 (0%)	0 (0%)	0 (0%)	0 (0%)	
<b>IIIC</b>	2(13.3%)	3 (60%)	1 (25%)	0 (0%)	0 (0%)	

MA:Macroadenoma, CP: Craniopharngioma, GL: Gliomas, GM: Germinoma, MG: Meningioma

\*Fisher-exact test, kruskal-Wallis test, Significant: P-value≤0.05, Non-significant: P-value>0.05.

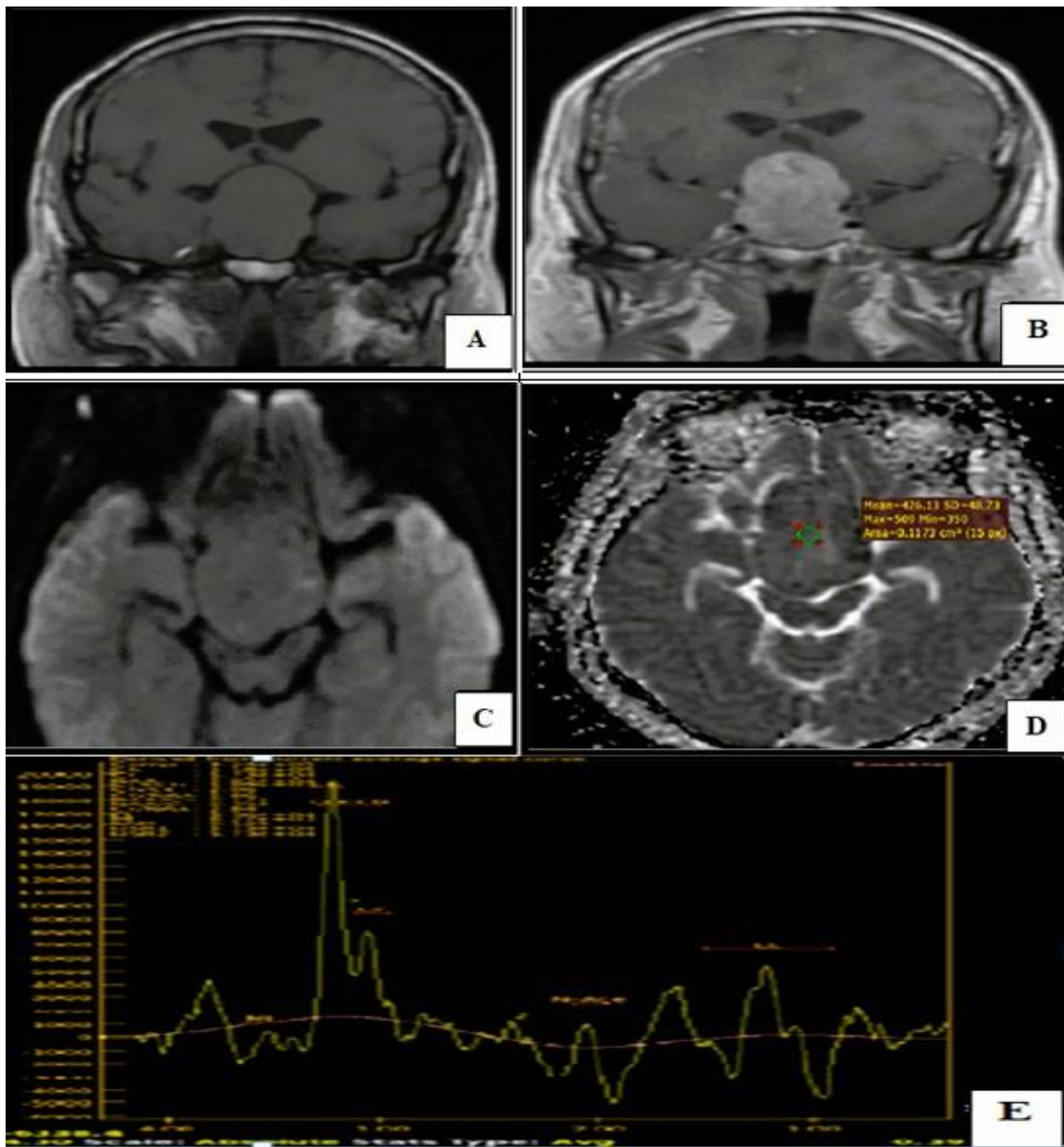


**Figure 1:** A 53 years old male patient, presented by headache & blurring of vision. Conventional MRI revealed Large fairly defined sellar and supra sellar mass lesion measuring about (51x47x38 mm),partially encasing the cavernous sinus with normal signal void ICA within, and significantly compressing the optic chiasm with no identified pituitary stalk **A**. Coronal T1WI: shows isointense signal relative to grey matter. **B**. Coronal post contrast T1WI: shows homogenous enhancement of the tumor. **C**. Axial DWI sequence (b =1000): shows isointense signal to the brain parenchyma. **D**. Axial ADC map: shows isointense signal to brain parenchyma with meanADC value (0.42) x 10<sup>-3</sup> mm<sup>2</sup>/s. **E**. MR spectroscopy (single voxel 1H-MRS): Pathological Type IIC spectrum with: shows significant reduction of NAA peak, Cr peak, moderate elevation of Cho, and a small Lip and Lac peak. MRI findings are consistent with Pituitary macroadenoma .Histopathology result was **pituitary Macroadenoma** .

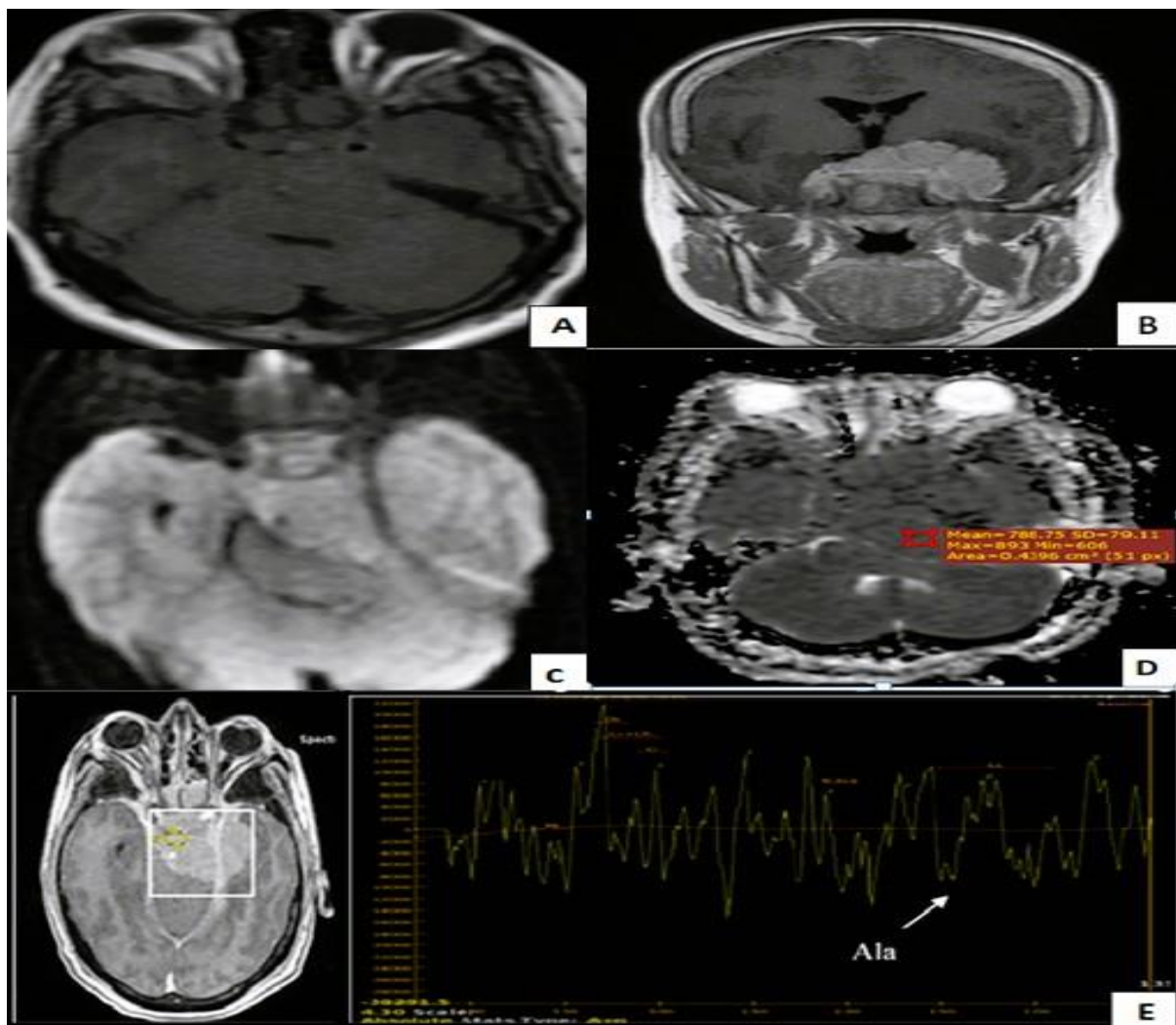


**Figure 2:** A 52 years old female patient presented by persistent headache & blurring of vision. Conventional MRI revealed a large fairly defined extra axial space occupying lesion seen occupying the sellar, supra-sellar, petro-clival and bilateral para-sellar regions (more at LT side). This lesion measuring 59 x 55 x 48 mm in maximum (TC, CC and AP dimensions) and extending laterally encasing bilateral cavernous sinuses with normal signal void ICA within more at left side and extending Superiorly and significantly compressing the optic chiasm and pituitary stalk.. **A.** Axial T1WI : shows isointense signal relative to grey matter. **B.** Coronal post contrast T1WI: shows intense homogenous post contrast enhancement with evidence of enhanced dural tail. **C.** Axial DWI sequence (b =1000): shows isointense signal compared to brain parenchyma. **D.** The axial ADC map: shows isointense signal compared to brain parenchyma with mean ADC value is  $(0.78) \times 10^{-3} \text{mm}^2/\text{s}$ . **E.** Spectroscopy (single voxel  $^1\text{H-MRS}$ ): Pathological Type IIC spectrum shows significant reduction of NAA peak, Cr peak, moderate elevation of Cho peak, small Lip and Lac peaks. The inverted doublet peak centered at approximately 1.49 ppm is consistent with an alanine (Ala) peak. MRI findings are consistent with large petro-clival, sellar and para-sellar meningioma. Histopathology result was **Meningioma**.

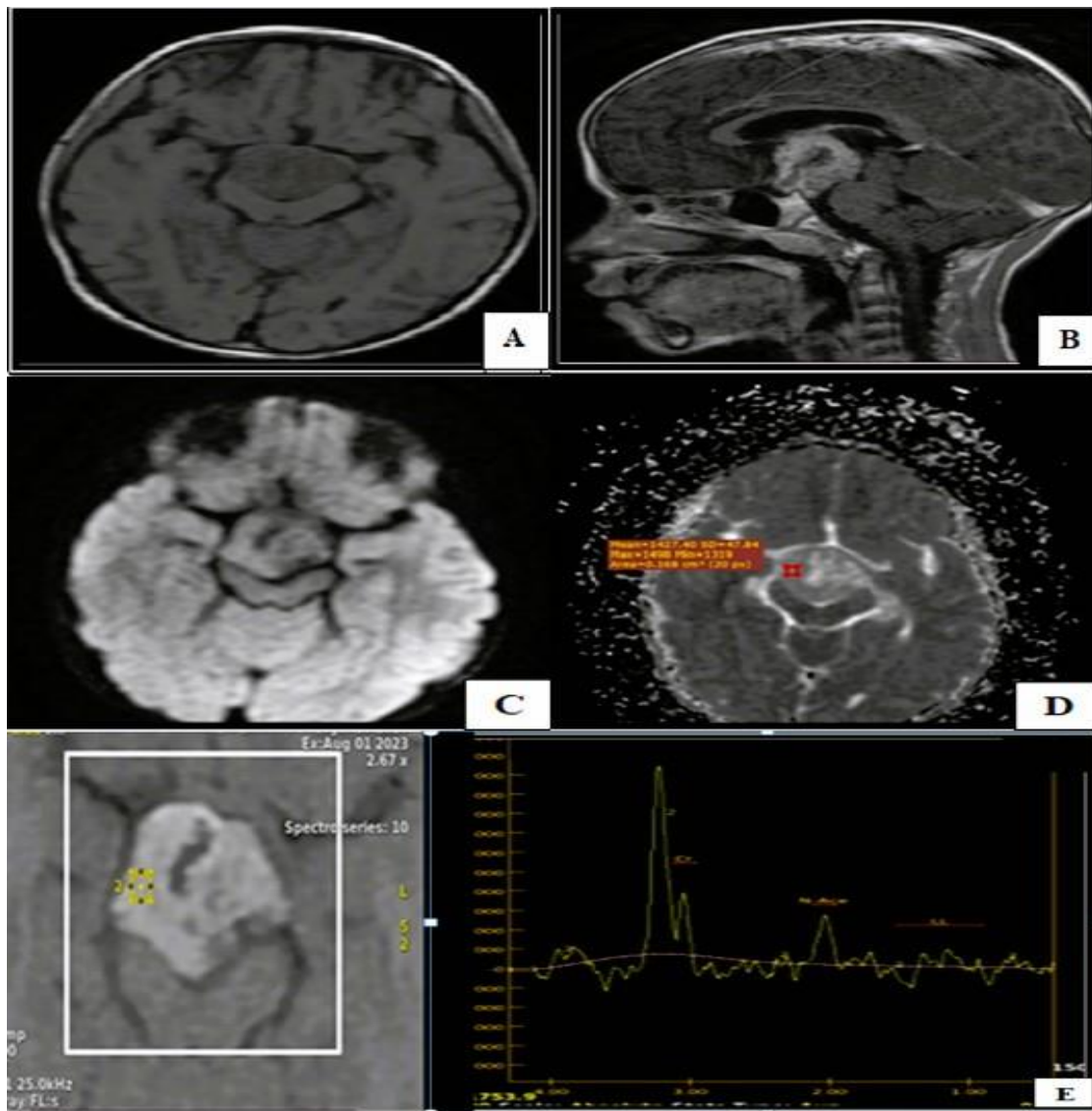


**Figure 3 :** A 5-year-old male patient presented by headache, blurring of vision.conventional MRI Revealed an ill-defined predominantly solid space occupying lesion at the supra sellar and 3rd ventricle region, it measures about 40 x 31 x 29 mm. **A.** Axial T1WI: shows hypointense signal relative to grey matter. **B.** Sagittal post contrastT1WI: shows moderate inhomogenous post contrast enhancement with small central cystic degeneration. **C.** Axial DWI sequence (b =1000): shows relative isointense signal to brain parenchyma. **D.** The ADC map: shows relative isointense signal to brain parenchyma with meanADC value is  $(1.42) \times 10^{-3} \text{ mm}^2/\text{s}$ . **E.** MR spectroscopy (single voxel 1H-MRS): Pathological Type IIC spectrum with: decrease of NAA peak, Cr peak, moderate elevation of Cho, and a small Lip and Lac peak. MRI findings are consistent with glioma.Histopathology result was **glioma**.

**DISCUSSION**

Suprasellar tumours are highly prevalent, and the most reliable method for identifying and diagnosing them is structural magnetic resonance imaging [8]. However, as the histopathology of the tumour may have a substantial impact on the surgical approach and treatment plan, it appears necessary to look for more diagnostic techniques for

tumour typing [8].

In our study we found pituitary adenoma as the most common lesion consisting (50%) of cases, which revealed a heterogeneous signal on DWI and different values for ADC conferring to their consistency. The ADC values calculated on ADC map, ranging from  $(0.4-1.1) \times 10^{-3} \text{ mm}^2/\text{s}$  with

mean ADC ( $0.72 \pm 0.25$ )  $\times 10^{-3}$  mm<sup>2</sup>/s. Among 15 patients diagnosed with macroadenomas, 6 patients (40%) had type IIC with moderate rise of lip, (20%) had type IA and IIC (**figure 1**) with mild lip elevation each, and only one patient (6.7%) had type IIIB. In harmony with previous reports of *Einstien et al.*, & *Chernov et al.*, [2,8] the majority of the macroadenomas 1H-MR spectra Type II, which was distinguished by significant decrease of NAA peak, moderate rise of Cho, residual Cr peak, and infrequent presence of small Lip and Lac peaks. Some authors as (*Einstien et al.*, *Chernov et al.* and *Kozicet al.*, *Mishra*) [2,8,9,10] stated that adenoma, originating from the adenohypophysis which does not infiltrate the brain and do not comprise neuroglial tissue, will not show any NAA resonances as well, as other extra cerebral tumors.

In the current study, there were 5 patients of craniopharyngiomas which represent (16.7%) of total patients with bimodal age distribution, 4 cases Out of the 5 were mixed cystic and solid lesions. Regarding the DWI craniopharyngiomas appeared hypointense with high ADC values in (80%) of cases. In the present study, average ADC values for craniopharyngiomas was ( $1.8 \pm 0.1$ )  $\cdot 10^{-3}$  mm<sup>2</sup>/s. in agreement with *Mohammad et al.* [11].

In our cases of craniopharyngioma we found MR spectra type IIIC in 3 cases (60%), our results were in accordance to *Einstien et al.*, & *Chernov et al.*, studies as they demonstrated that craniopharyngiomas are typically depicted by pathological 1H-MR spectra Type III C with considerable reduction of all metabolites and existence of several additional peaks. It seems, that such metabolic pattern caused by existence of microcysts and calcifications within the examined tissue volume, as no voxel contamination was revealed in any of these cases, [2,8].

*Sener RN.*, investigated the cyst fluid of craniopharyngeomas and found a characteristic prominent broad peak of Lip was met at 1.3 ppm. He correlated it with the histologic conclusions showing high amounts of cholesterol in the fluid in the cyst [12]. In our study, we didn't examine any cysts. We put the voxel on the solid portions of the tumor averting any cystic components.

Among the 4 cases of gliomas histopathology proved grade I in 3 cases (pilocytic astrocytomas) and one case of high grade glioma, (50%) of them were hypointense on DWI and hyperintense on ADC map with mean ADC ( $1.38 \pm 0.5$ )  $\times 10^{-3}$  mm<sup>2</sup>/sec (**figure 3**).

Our results are in accordance with *Panyaping et*

*al.* who found that mean ADC values in chiasmatic/hypothalamic gliomas CHG is ( $1.43 \pm 0.3$ )  $\times 10^{-3}$  mm<sup>2</sup>/sec [13].

MR pathological spectra for our glioma cases were characterized by increase of Cho peak and decreased NAA, Cr peaks. Three tumors had pathological 1H-MR spectra type II: (2 IIC with mild lip elevation, one patient had type IIC with moderate lip elevation) and one patient had type IIIC. A similar findings reached by, *Einstien et al.*, & *Shiroishi et al.*, found that most of their cases had pathological Type II spectrum, although he identified NAA in some gliomas and speculate that can be due to either presence of viable neurons within the bulk of neoplasm and infiltrative growth of the tumor or by production of the metabolite by the neoplastic cells itself [2, 14].

Among 10% of our meningioma cases, there was no diffusion restriction on DWI and the mean ADC value was  $0.94 \pm 0.16 \times 10^{-3}$  mm<sup>2</sup>/sec.

Regarding MRS in our results, the diagnosis of meningioma was suggested in 2 cases out of 3 as they displayed type IIC spectrum with an raised Alanine peak (at 1.49 ppm) as in case in **figure 2** while the third case revealed characteristic type IIC with no alanine peak. Other studies [2, 8, 11, 15, 16] agree with us regarding the vast majority of meningioma displayed type II C spectrum with raised alanine peak (at 1.49 ppm).

In the existing study, there were 3 patients of germinomas which represented (10%) of total patients, most of germinoma cases (66.7%) were hyperintense on DWI with restricted diffusion, the average ADC values for geminoma was  $0.80 \pm 0.2 \times 10^{-3}$  mm<sup>2</sup>/s. *Yamasak et al.*, *Ogiwara et al.*, *Douglas-Akinwande et al.*, *Panyaping et al.*, demonstrate that high intensity on DWI and lower ADC is characteristic of germinoma [17,18,19,2].

Among the three patients diagnosed with germinoma, 2 patients had type IIC with moderate lip elevation and one patient had type IIIA (predominant peak was Lip then Cho). *Chernov et al.*, and *Mohammad et al.*, reported that germinoma is typically characterized by decreased to absent NAA & Cr peaks with significant elevation of Cho and moderate to marked elevation of Lip peak (type II C spectrum). Taking into consideration that in both studies only small number of germinoma was investigated [8,11]. *Yamasaki et al.*, study demonstrates that germinoma tumors expressed high lipids peak and consider that the mechanisms for recognition of high lipids peak in germinoma arise not from necrosis but from other two

mechanisms: infiltrating lymphocyte and apoptosis of tumor cells [17].

The pathological 1H-MR spectra over the sellar and suprasellar masses were in line with the MRS findings of brain neoplasms in the literature, we observed that NAA was markedly reduced whenever brain tissue was spoiled or substituted by any process. Extraaxial lesions which do not comprise neuroglial tissue or infiltrate brain, didn't demonstrate NAA resonances. Increased Cho was observed in processes with increased cell-membrane turnover and alanine was the most characteristic metabolite of meningioma.

This study had some limitations: Firstly, the number of patients was quite small. More studies may require a greater number of patients. Secondly susceptibility artifacts of sellar and parasellar lesions cause image disruption on DWI sequences, resulting in inadequacy in ADC value measurement. We recommend further studies with PROPELLER non-EPI DWI technique for better evaluation. Thirdly, limitation of practical use of 1H-MRS only to tumors with significant suprasellar extension owing to relatively large size of the voxel clinical MR imagers with magnetic field strength of 1.5 Tesla. Finally, there is definite disparity of the metabolic patterns in neoplasms with similar histological type, whereas more or less similar neurochemical alterations can be noted in entirely diverse diseases. In further studies, we can enhance diagnostic efficacy of spectroscopic neuroimaging with higher magnetic field strength (3 Tesla and more).

### CONCLUSIONS

Diffusion-weighted MRI and MR Spectroscopy can provide valuable information, which may be effectively used complementary to conventional MRI examination and contribute to presurgical evaluation and distinction between diverse sellar, suprasellar masses.

### ABBREVIATIONS

**ADC:** Apparent diffusion coefficient ;**Cho:** Choline ;**CP:** Craniopharyngioma ;**Cr:** Creatine; **DCE-MRI:** Dynamic contrast-enhanced magnetic resonance imaging; **DWI:** Diffusion-weighted MR imaging; **FLAIR:** Fluid attenuated inversion recovery; **FOV:** Field of view; **1H MRS :**Proton Magnetic Resonance Spectroscopy; **ROC :**Receiver- operator characteristic curve; **ROI:** Regions of interest; **SE:** Spin echo sequence; **sec:** Second; **SI:** Signal intensity T1WIT1-weighted image;**T2 TSE:**T2-weighted turbo spin-echo;**T2WI:**T2-weighted

image; **TE:** Echo time; **TR :**Repetition time

### REFERENCES:

1. **Batra V, Gupta P K, Gehlot R, and Awasthi P.** Radiopathological correlation of sellar and suprasellar masses: Our experience. *Int J Res Med Sci* 2016; 4(9): 3924-8.
2. **Einstien A, and Virani R A.** Clinical relevance of single-voxel 1H Mrs metabolites in discriminating suprasellar tumors. *Journal of clinical and diagnostic research: JCDR* 2016; 10(7): TC01.
3. **Hu X, Xue M, Sun S, Zou Y, Li J, Wang X , et al.** Combined application of MRS and DWI can effectively predict cell proliferation and assess the grade of glioma: a prospective study. *J. Clin. Neurosci.* 2021; 83: 56-63.
4. **Aydın Z B, Aydın H, Birgi E, and Hekimoğlu B.** Diagnostic value of Diffusion-weighted Magnetic Resonance (MR) imaging, MR Perfusion, and MR Spectroscopy in addition to Conventional MR imaging in Intracranial Space-occupying Lesions. *Cureus* 2019; 11(12).
5. **Yamasaki F, Sugiyama K, and Kurisu K.** Brain Tumors: Apparent Diffusion Coefficient at Magnetic Resonance Imaging. *Methods of Cancer Diagnosis, Therapy, and Prognosis: Brain Cancer* 2011; 279-96.
6. **Makada M, and Matang M.** Role of DWI in intracranial pathologies with its comparison to flair and T2w imaging. *Int J Acad Med Pharm* 2023; 5(1): 433-47.
7. **Sohu D M, Sohail S and Shaikh R.** Diagnostic accuracy of diffusion weighted MRI in differentiating benign and malignant meningiomas. *Pak. J. Med. Sci.* 2019; 35(3): 726.
8. **Chernov M F, Kawamata T, Amano K, Ono Y, Suzuki T, Nakamura R, et al.** Possible role of single-voxel 1 H-MRS in differential diagnosis of suprasellar tumors. *J. Neurooncol.* 2009; 91: 191-8.
9. **Kozic D, Medic-Stojanoska M, Ostojic J, Popovic L, and Vuckovic N.** Application of MR spectroscopy and treatment approaches in a patient with extrapituitary growth hormone secreting macroadenoma. *Neuro endocrinol. Lett.* 2007; 28(5): 560-4.
10. **Mishra G V, Gowda K H, Bhansali P J, Nagendra V, and Raj N.** Pituitary Macroadenoma–Evaluation of Mean Metabolic Ratios and Mean and Normalized Apparent Diffusion Coefficient Values Using Magnetic Resonance Spectroscopy and Diffusion-weighted

Imaging in a Central Indian Rural Hospital Setup. *J. Datta Meghe Inst. Med. Sci.* 2022; 17(4): 838-41.

**11.Mohammad, F.F, Hasan, D.I, and Ammar M G.** MR spectroscopy and diffusion MR imaging in characterization of common sellar and suprasellar neoplastic lesions. *EJRN* 2014; 45(3): 859-67.

**12.Sener RN.** Proton MR spectroscopy of craniopharyngiomas.*CMIG* 2001; 25(5): 417-22.

**13.Panyaping T, Taebunpakul P and Tritanon O.** Accuracy of apparent diffusion coefficient values and magnetic resonance imaging in differentiating suprasellar germinomas from chiasmatic/hypothalamic gliomas.*NRJ* 2020; 33(3):.201-9

**14. Shiroishi M S, Panigrahy A, Moore K R, Nelson M D, Gilles F H, Gonzalez-Gomez, I, et al.,** Combined MRI and MRS improves pre-therapeutic diagnoses of pediatric brain tumors over MRI alone. *Neuroradiology* 2015; 57: 951-6.

**15.Kabir Z, and Sohely M.** Sensitivity and Specificity of Magnetic Resonance Spectroscopy (MRS) in the Diagnosis of Meningiomas. *AJORRIN* 2023; 6(1): 194-205.

**16.Dahamou M, Bakkar N, Dehenh Y, Khouali M, Oulali, N, and Moufid F.** Atypical radiological

aspect of meningioma: Web-like enhancement. *Radiol. Case Rep.* 2023; 18(8): 2796-9.

**17.Yamasaki F, Kinoshita Y, Takayasu T, Usui S, Kolakshyapati M, Takano M, et al.** Proton magnetic resonance spectroscopy detection of high lipid levels and low apparent diffusion coefficient is characteristic of germinomas. *World Neurosurg.* 2018; 112 : 84-94.

**18.Ogiwara H, Tsutsumi Y, Matsuoka K, Kiyotani, C, Terashima K, and Morota, N.** Apparent diffusion coefficient of intracranial germ cell tumors. *J. Neurooncol.* 2015; 121: 565-71.

**19.Douglas-Akinwande A C, Ying J , Momin Z , Mourad A, and Hattab E M.** Diffusion-weighted imaging characteristics of primary central nervous system germinoma with histopathologic correlation: a retrospective study. *Acad. Radiol.* 2009; 16(11): 1356-65.

**20.Panyaping T, Tritanon O, Wisetsathon P, Chansakul T, & Pongpitcha P.** Accuracy of apparent diffusion coefficient values for distinguishing between pineal germ cell tumour and pineoblastoma. *Clin. Radiol.* 2023; 78(7): 494-501.

### To Cite :

**Hassan, R., Ragheb, A., Elmajdub, S., Almolla, R. Complementary Effect Of Diffusion MR Imaging and Single-Voxel 1H MR Spectroscopy Metabolites in Charachterization Of Sellar and Suprasellar Masses. Zagazig University Medical Journal, 2024; (422-432): -. doi: 10.21608/zumj.2024.259344.3089**